NOVEL CURRENT LINE SENSOR BASED ON MATCHED OPTOCOUPLERS FOR ACTIVE POWER FACTOR CORRECTION

Paul MĂRTARI, Dorin PETREUS, Marius NEAG
Technical University of Cluj-Napoca, Cluj-Napoca, Romania
email: Marius.Neag@bel.utcluj.ro

Abstract: This paper presents a novel line current sensor which allows safe and accurate data acquisition for power factor measurements: it uses a pair of matched optocouplers arranged so that the difference between their outputs is proportional with the line current; thus the second order harmonics caused by the inherent non-linearity of the optocouplers are cancelled. A system for analyzing experimentally the effects the power factor (PF) has over the efficiency of quasi-resonant flyback switch mode power supplies (SMPS) was build based on this sensor. It provides the chronograms of the line voltage and current, along with the most important data related to the power factor and the efficiency of the power conversion. Experimental results shows that active power factor correction improve the efficiency of the SMPS by up to 6%.

Keywords: *Line Current Sensor, Power Factor Correction, Quasi-resonant Flyback Converter*

I. INTRODUCTION

Designers of switch-mode power supplies (SMPS) are usually required to minimize the effects the SMPS high level of harmonic distortion and electro-magnetic interference (EMI) have on the main supplying grid. The EU standard EN61000-3-2 requires that all SMPS with output power of at least 75 W must include active power factor correction (PFC), in order to maintain the power factor (PF) level above 0.9. Early solutions, based on low cost passive LC filters and Valley-Fill filters, are suited mainly for small power consumers like the compact fluorescent light (CFL) bulbs, with rated power usually under 50W. Typically, passive PFC can provide a power factor value of around 0.8; this can be pushed to over 0.9 if larger, more complex – thus more expensive – filters are used [1].

Sensing the line current is essential for PFC monitoring but for several types of SMPS, such as the quasi resonant flyback converter, implementing the line current monitors is quite difficult. The main problem there is the high level of the line voltage that often requires galvanic separation. The measurement frequency domain needs to include not only the grid frequency but also the harmonic components. Classical current transformers-based solutions have relatively small bandwidths close to the grid frequency which makes them unsuitable for PF measurements [2]. Other current sensors employ the Hall effect [3]; in general, they are best suited for high power applications as they present a dead zone near zero, i.e. their output is not accurate/valid for low current levels [2], [3].

Current sensor based on optocouplers, with current shunt sense resistor topology, can avoid these drawbacks. The relatively low voltage drop across the sense resistor can be gained up using various strategies, such as a DC isolation amplifier in [4]. The effects of the optocoupler nonlinearity and ageing can be reduced by placing them within the feedback loop of an operational amplifier. The main drawbacks of such implementations are their reliance on the power supply symmetry and thee fairly complex circuitry they require. The solution proposed in [5] avoids the symmetric power supply requirement but it is limited to unidirectional (DC) current sensing.

The novel current sensor presented in Section IV of this paper overcomes all the drawbacks mentioned above. Based on it, a system for measuring accurately the PF in SMPS was designed and implemented. It was validated by both simulation results and experimental measurement.

II. ACTIVE POWER FACTOR CORRECTION FOR SYSTEMS WITH NON-LINEAR LOADS

A. SYSTEMS WITH NON-LINEAR LOADS

If the PF value is not equal to 1, the current waveform does not follow the voltage waveform. This result not only in power losses, but may also cause harmonics that travel down the neutral line and disrupt other devices connected to the line. The closer the PF value gets to 1, the closer to zero the current harmonics will get, since then most of the power will be at the fundamental frequency. When the current is not sinusoidal and the voltage is sinusoidal, the power factor consists of two factors: 1) the displacement factor ($K_{Ø}$) related to the phase angle and 2) the distortion factor (K_D) related to the shape of the wave. The expression of the total PF as a function of the displacement and distortion factors is [6]:

$$\mathrm{PF} = K_D K_\theta = \frac{I_{\mathrm{RMS1}}}{I_{\mathrm{RMS}}} \cdot \cos(\theta) = \frac{1}{\sqrt{1+\mathrm{THD_I}^2}} \cdot \cos(\theta) \quad (1)$$

where $\mathrm{THD_I}$ is the total harmonic distortion of the load current, I_{RMS1} is the fundamental component of the current and the I_{RMS} is the current RMS value. Therefore, the purpose of the power factor correction circuit is to minimize the input current distortion and make the current in phase with the voltage.

A particularly important class of non-linear loads comprises the billions of personal computers, laptops and TV monitors that incorporate switch-mode power supplies. The majority of low cost power supplies contain a simple full-wave rectifier that conducts only when the mains instantaneous voltage exceeds the voltage on the main input capacitors. Thus the input current is distorted, with a significant part of its energy spread over a large

Manuscript received June 25 2013; revised September 25 2013

number of harmonics. The peak to average ratio of the input current is very large, which means the distortion power factor, K_D, has low values; all these yield a rather poor PF.

In order to reduce the pollution of the main power supply such a non-linear load can cause one should monitor and actively correct the PF.

B.ACTIVE POWER FACTOR CORRECTION

An active power factor corrector (active PFC) is a power electronic system that changes the shape of the current waveform drawn by a load in order to improve the power factor. In general, for a switched-mode power supply with active PFC, a boost converter - called the PFC preconverter in Figure 1 - is placed between the bridge rectifier and the main input capacitor. The boost converter attempts to maintain a constant DC bus voltage on its output while drawing a current that is proportional with and has the same frequency, phase and shape, as the line voltage. For example, SMPS with passive PFC can achieve power factor of about 0.8, SMPS with active PFC, up to 0.99 power factor, while a SMPS with no PFC has a power factor value of around 0.6 [1] [7].

III. SYSTEM FOR ACCURATE MEASUREMENT OF THE POWER FACTOR IN SMPS

Figure 1 presents the block diagram of a data acquisition system for measuring accurately the PF in SMPS. This system was used to study the effect the PF has on a quasi-resonant flyback converter. The focus of this paper is the Line Current Sensor block; its main components are illustrated in the Figure: a sense resistor placed in series with the line voltage, an auxiliary voltage source (V_{AUX}) supplied by the line voltage and an optocoupler based transducer that ensures the galvanic separation between the line voltage and the output signal. The current sensor block is followed by the bridge rectifier, with a small-value high frequency bypass capacitor at its output. The PFC Preconverter block illustrates the boost principle of DC-DC conversion along with a large value bulk storage capacitor. In the right side of the block diagram, a SMPS Converter block is shown, representing here the flyback converter. The block placed at the bottom of the diagram highlight the fact that data acquisition is realized using National Instruments (NI) hardware and processed with the LabView interface software. The convertor is built around Fairchild's FAN6920 controller, which comprises a Boundary Conduction Mode PFC controller and a Quasi-Resonant (QR) PWM controller [8]. The hardware also includes the NI DAQ for data acquisition while the software was developed in the LabView environment.

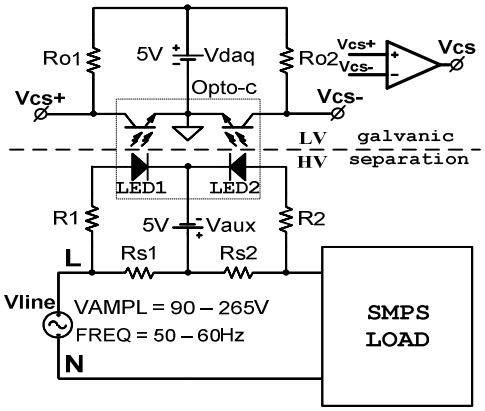

Figure 2: Simplified schematic of the proposed line current sensor based on matched optocouplers.

IV. A NOVEL LINE CURRENT SENSOR

Most of the existing line current sensors cannot operate at the frequency levels commonly used in SMPS, hindering THD measurements. Also, having a current sensor with galvanic separation is essential for safe measurements.

Both the wide frequency range and galvanic separation are provided by the line current sensor based on optocouplers proposed in Fig.2. Its main idea is to reduce/minimize the 2nd order harmonics introduced by the nonlinearity of the optocouplers by using a matched pair of optocouplers arranged so that the difference between the voltages at their outputs is proportional with the line current.

The proposed current sensor operates as follows: when the line current flows through R_{s1} and R_{s2}, the voltage across these resistors will cause signal currents of opposite sign to appear in the optocoupler LEDs, on top of their biasing current which is provided by the DC source V_{AUX}. At the output of the two optocouplers the signal currents through LED_1 and LED_2 appear amplified by the optocouplers' gain, K_{CTR}. As a result, the voltages V_{CS+} and V_{CS-} developed across resistors R_{o1} and R_{o2} are proportional with the line current but 2nd order harmonics appear in their spectrum due to optocouplers' nonlinearity, as shown in Fig.3. To overcome this problem, the difference between V_{CS+} and V_{CS-}, called hereafter the V_{CS} voltage, is used to derive the line current; it has a cleaner spectrum characteristic, as seen in the zoom-in area of Fig.3. The resulting V_{CS} voltage is proportional with the line current:

$$V_{CS} = V_{CS+} - V_{CS-} = \frac{R_{S1,2}}{R_{1,2}} \cdot 2 I_{LINE} K_{CTR} R_{O1,2} \qquad (2)$$

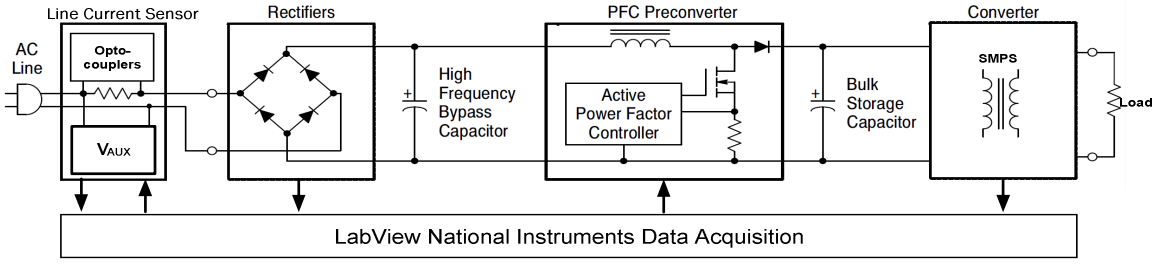

Figure 1: Block diagram of a typical SMPS with the system used for measuring accurately its Power Factor; the later comprises the line current sensor proposed here and National Instruments data acquisition hardware and soft tools.

A supplementary voltage source - called V_{DAQ} in Fig.2 - is used for biasing the output stage of the optocouplers; in this system it is supplied by the data acquisition board, hence the name.

One can see that the auxiliary voltage supply, V_{AUX}, is placed in a somewhat un-conventional connection: its positive terminal is connected to the line voltage through R_{s1}. This connection is made in order to obtain the floating DC voltage source necessary to bias the optocoupler LEDs. Despite this connection the arrangement remains safe for the user, who has to deal only with the voltages V_{CS+} and V_{CS-}, which are on the other side of the galvanic insulation provided by the optocuplors from the line voltage and the V_{AUX} source.

V. SIMULATION RESULTS

Simulations were run with the LTspice software on a testbench derived from Fig.2: the voltage sources V_{AUX} and V_{DAQ} were set to 5V. The bias current through the optocuplor LEDs is set to 10mA by resistors R_1 and R_2, of 750Ω each. To maximize the output voltage swing of V_{CS+} and V_{CS-} their common-mode level is set to half of V_{DAQ} by resistors, R_{O1} and R_{O2}, here of 330Ω each. The value of the sense resistors $R_{S1,2}$ was chosen to be 0.47Ω. A model provided by the manufacturer was used for the optocouplers.

Figure 3 presents the spectra of the main voltages in the system: the line voltage V_{Line} with the fundamental frequency of 50Hz; the voltages at the output of the two optocuplors, V_{CS+} and V_{CS-}, which are overlapped over the entire frequency range with the exception of the zone around 100Hz (second harmonic) and the voltage V_{CS}, the difference between V_{CS+} and V_{CS-}.

The zoom-in on the top right of Fig.3 demonstrates the efficiency of the proposed differential measurement in eliminating the second-order distortions. Note that in this simulation optocuplors were assumed perfectly matched; the inherent mismatches of a real-life implementation will prevent the complete elimination of these distortions but they will be significantly reduced.

Figure 4 shows the simulated transfer function of the sensor; this curse is in good agreement with eq. (2) over a fairly large range of I_{Line} values. By comparing the $V_{CS}(I_{Line})$ curve against the ideal line one obtains the systematic error of the proposed sensor. This error is very small for about half the I_{Line} range considered in this

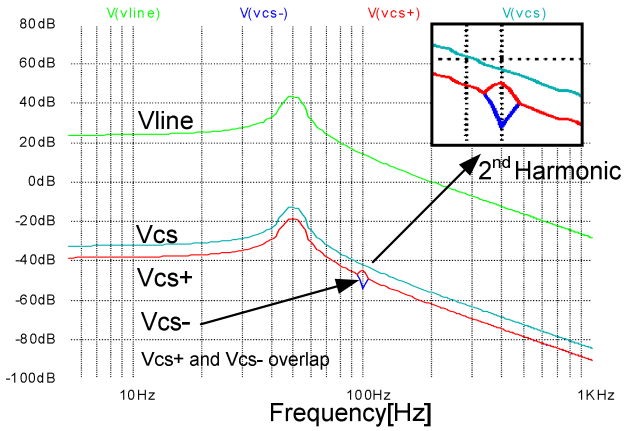

Figure 3. FFT analysis, Hamming Window, for V_{CS}, V_{CS+}, V_{CS-}, I_{Line} around I_{Line}=1A, 50Hz, Pure resistive load.

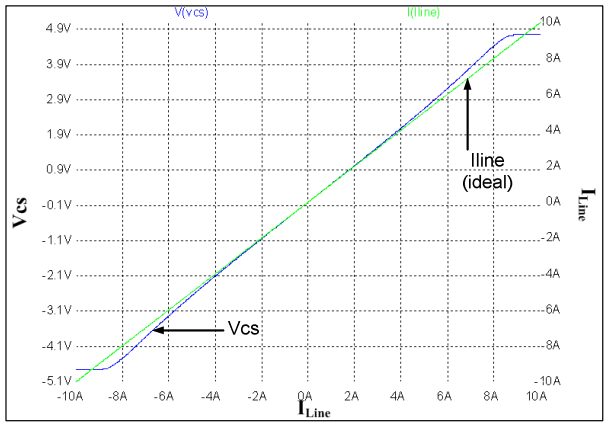

Figure 4:Transfer characteristic of the current sensor.

simulation, and then increases to about 10% at the point where the sensor saturates – here at 8A. The saturation limit depends mainly on the supply voltage V_{DAQ} and the maximum and minimum current levels through the LEDs.

Besides the errors shown in these simulation results one should also expect some gain error due to the ageing of the optocouplers, that leads to the degradation of their K_{CTR} over time. A calibration procedure should be considered if one needs accurate measurements outside the range for which the sensor error is inherently small (in this example +/-5A) and/or for dealing with the ageing effects; an example will be presented in Section VI.

VI. EXPERIMENTAL RESULTS

A. THE TEST SETUP

A test setup was built following the block diagram shown in Fig.1; the SMPS that represents the non-linear load was a fly-back converter implemented with the FAN6920 controller; it was designed for a maximum output power of 80W with a rated output voltage of 19V. The experimental setup also includes a standard line filter and a Π filter which are not illustrated in Fig.1. A transformer with variable output voltage was used to implement the AC line in a safe and controlled way.

Data acquisition was performed by using the DAQ interface from National Instruments, driven by a program developed in LabView, which performs data processing and ensures the interface with the user.

A real-life implementation of the current sensor proposed in Fig. 2 was built in order to perform lab experiments; all circuit elements have the same values as the ones used in the simulations described in the previous Section. Thus, one can compare directly the actual measurements with the simulation results.

The main circuit component is the HCPL2531 double optocoupler IC. The biasing voltage source V_{DAQ} in Fig. 2 was supplied by the DAQ interface. Low-tolerance resistors were used for precise measurements.

For each lab experiment measurement the voltages V_{CS+} and V_{CS-} are measured and converted in digital representation by the DAQ interface; these data are then processed automatically by a program written in LabView which derives the line current value. The data processing software also implements a simple yet effective calibration procedure of the systematic error of the

transfer characteristic seen in Fig. 4: an additional calibration factor, K_{CAL}, is introduced in eq. 2, so that the line current is obtained from the following equation:

$$I_{LINE} = \frac{V_{CS}}{2 \cdot K_{CTR} R_{O1,2}} \frac{R_{1,2}}{R_{S1,2}} \cdot K_{CAL} \qquad (3)$$

A set of reference measurements is performed with the proposed sensor, then with standard lab equipment; by comparing the results one can derive the value of K_{CAL}.

A photo of the test setup is shown in Figure 6; the main elements are highlighted for easier identification: the NI DAQ, the main capacitor, the SMPS and transformer and PFC controller, the PFC inductor, the line and Π filters, the auxiliary voltage source V_{AUX} and the matched optocoupler IC. The circuit implementation was realized on a generic 2.54mm matrix holes test board; the relative positioning of main components was done carefully in order to minimize the electro-magnetic interference; however, this topic is outside the aim of this paper.

B. A SELECTION OF LAB MEASUREMENTS

Results of a typical experiment are presented in the followings. The line AC voltage and the SMPS output power are set to known values - here 110V and 40W, respectively. The data acquisition system described above monitors the time evolutions of the line voltage and current for various settings and presents them graphically.

For example, the chronograms shown in Figures 6 and 7 were obtained with the Active PFC enabled (Fig. 6) and disabled (Fig. 7). They illustrate the strong influence the shape of the AC line current has on the power factor value: with the active PFC disabled, the shape of the current presents spikes with large amplitude - 2.2A- and the resulting value of the PF is rather poor, at 0.72; with the PFC enabled, the shape of the current waveform is close to the voltage line, with a peak amplitude of only 0.6A, and the PF value improves dramatically, to 0.998.

The graphic interface used for results interpretation, also presents detailed information on the power factor components: Distorted PF, Displacement PF, phase shift, AC line voltage and current THD; data on the efficiency of the entire power conversion system are also available.

Table 1 summarizes the data obtained for the experiment described above, along with data obtained for a similar experiment but with the line voltage set to 230V.

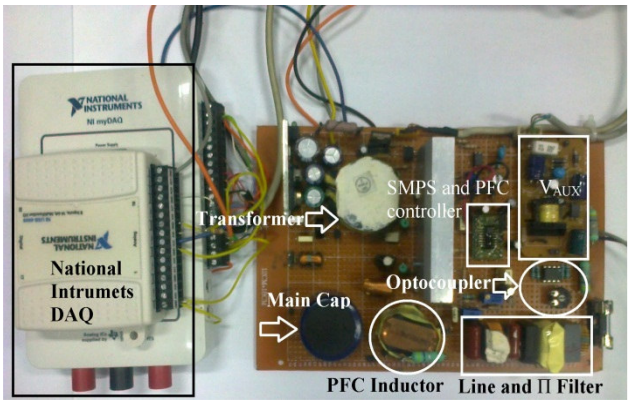

Figure 5. Photo of the test setup used for lab experiments; the main components of the test board are identified

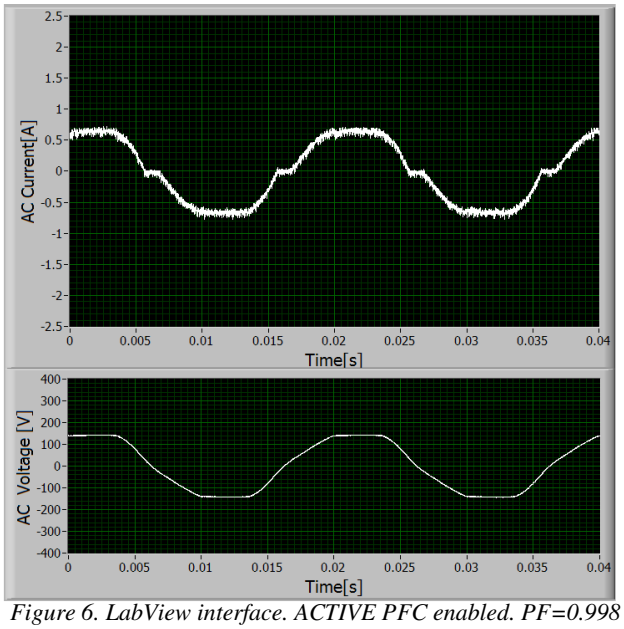

Figure 6. LabView interface. ACTIVE PFC enabled. PF=0.998

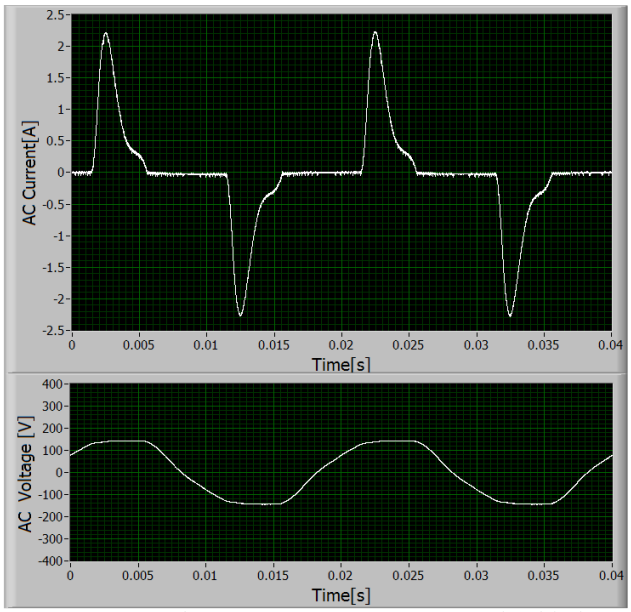

Figure 7. LabView interface. Active PFC disabled. PF=0.72

It is worth noting that, despite the fact that the active PFC boost converter has sub unitary efficiency, it has significant effect on the efficiency of the overall power conversion system. When the PFC is disabled, the large

Table 1: Summary of data provided by the proposed system for two experiments; note the PF influence over efficiency

Active PFC	OFF	ON	OFF	ON
Input Voltage	110Vac		230Vac	
Displacement PF	0.985	0.998	0.999	0.983
Distortion PF	0.734	0.999	0.798	0.998
Total PF	0.724	0.998	0.798	0.982
Efficiency [%]	74.50%	82%	74.50%	80.20%
Output Power	40W			

RMS value of the input current degrades the efficiency of the rectifier and a large amount of power is wasted in harmonic components. When enabled, the PFC reduces the level of the input current absorbed from the grid and the power loses in harmonic components.

Obviously, the current spikes shown in Fig. 7 distort the line voltage, the measured THD of the later getting close to 10% in this case. This has a significant impact on the measurement of the distortion power factor, K_D, which can be expressed as follows[6]:

$$K_D = \frac{1}{\sqrt{1+\mathrm{THD_I}^2}} \quad (4)$$

To overcome this problem the THD of the measured current was normalized with respect to the THD of the AC input voltage:

$$\mathrm{THD_{I(NORM)}} = \mathrm{THD_{I(AC)}} - \mathrm{THD_{V(AC)}} \quad (5)$$

where $\mathrm{THD_{I(NORM)}}$ represents normalized value of the current THD used in (4), $\mathrm{THD_{I(AC)}}$ is the measured value of the line current THD and $\mathrm{THD_{V(AC)}}$ is the measured value of the line voltage THD.

VII. CONCLUSIONS

A novel line current sensor based on optocouplers has been proposed and demonstrated both in simulations and in a real-circuit implementation. Its main idea is to reduce/minimize the second order harmonic introduced by the inherent nonlinearity of the optocouplers by using a matched pair of optocouplers arranged so that the difference between the voltages at their outputs is proportional with the line current.

This line sensor was used to implement a test setup for studying the effects the power factor has over the efficiency of quasi-resonant flyback switch mode power supplies. The test setup also comprises a data acquisition system based on the DAQ interface from National Instruments, driven by a program developed in LabView, which also performs data processing and ensures the interface with the user. This system is able to monitor the time evolutions of the line voltage and current and to present them graphically, along with the most important data of the power conversion: the power factor and its components (the distorted PF and the displacement PF), the phase shift, the THD of the AC line voltage and current THD, the overall efficiency of the conversion.

Experimental results show that by using active power factor correction one can push the power factor level up to 0.999, thus improving the efficiency of the SMPS by up to 6%.

ACKNOWLEDGMENTS

The first author wishes to thank Silicon Systems Transylvania Ltd. for their granting him a generous scholarship throughout his M.Sc. studies.

REFERENCES

[1] H. Z. Azazi, E. E. EL - Kholy, S. A. Mahmoud and S. S. Shokralla. (MEPCON'10) "Review of Passive and Active Circuits for Power Factor Correction in Single Phase, Low Power ACDC Converters"

[2] Teridian Semiconductor Corporation AN_661x_021, "Using Current Transformers with the 78M661x." Available: http://pdfserv.maximintegrated.com/en/an/AN4841.pdf

[3] Paul Emerald, "Non-Intrusive Hall-Effect Current-Sensing Techniques Provide Safe, Reliable Detection and Protection for Power Electronics".
Available:
http://www.allegromicro.com/~/media/Files/Technical-Documents/STP98-1-Non-Intrusive-Hall-Effect-Current-Sensing-Techniques.ashx

[4] Agilent Technology, Linear Applications of Optocouplers. Application Note 951-2.
Available: www.avagotech.com/docs/5954-8430E.

[5] Roger Griswold, "AP1867-Optocoupler Extends High-Side Current Sensor".
Available: http://www.maximintegrated.com/app-notes/index.mvp/id/1867

[6] Gonzalo Sandoval, "Power Factor in Electrical Power Systems with Non-Linear Loads", ARTECHE / INELAP S.A.
Available:
http://www.artechepq.com/assets/files/PF_nonlinearloads.pdf

[7] Sugawara, I., Suzuki, Y., Takeuchi, A., & Teshima, T, "Experimental studies on active and passive PFC circuits,
By: Sugawara, I., Suzuki, Y., Takeuchi, A., & Teshima, T".

[8] "FAN6020MR mWSaver Technology Integrated Critical-Mode PFC and Quasi-Resonant Curent-Mode PWM Controller"
Available:
http://www.fairchildsemi.com/pf/FA/FAN6920MR.html

[9] "Application Note 42047 Power Factor Correction (PFC) Basics". Fairchild Semiconductor (2004). Available: http://www.fairchildsemi.com/an/AN/AN-42047.pdf

[10] "Power Factor Correction Handbook". ON Semiconductor (2007). Available:
http://www.onsemi.com/pub_link/Collateral/HBD853-D.PDF

[11] "Linear Applications of Optocouplers. Application Note 951-2". Available: www.avagotech.com/docs/5954-8430E.